Available online at www.sciencedirect.com
ScienceDirect
Current Opinion in
Electrochemistry

Review Article

Progress of transition metal chalcogenides as efficient electrocatalysts for energy conversion

Manashi Nath, Harish Singh[a] and Apurv Saxena[a]

Abstract
The continuous excessive usage of fossil fuels has resulted in its fast depletion, leading to an escalating energy crisis as well as several environmental issues leading to increased research towards sustainable energy conversion. Electrocatalysts play crucial role in the development of numerous novel energy conversion devices, including fuel cells and solar fuel generators. In particular, high-efficiency and cost-effective catalysts are required for large-scale implementation of these new devices. Over the last few years, transition metal chalcogenides have emerged as highly efficient electrocatalysts for several electrochemical devices such as water splitting, carbon dioxide electroreduction, and, solar energy converters. These transition metal chalcogenides exhibit high electrochemical tunability, abundant active sites, and superior electrical conductivity. Hence, they have been actively explored for various electrocatalytic activities. Herein, we have provided comprehensive review of transition-metal chalcogenide electrocatalysts for hydrogen evolution, oxygen evolution, and carbon dioxide reduction and illustrated structure–property correlation that increases their catalytic activity.

Addresses
Department of Chemistry, Missouri University of Science & Technology, Rolla, MO, 65409, USA

Corresponding author: Nath, Manashi (nathm@mst.edu)
[a] Equal contribution.

Current Opinion in Electrochemistry 2022, **34**:100993
This review comes from a themed issue on **Electrocatalysis**
Edited by **Nicolas Alonso-Vante**
For a complete overview see the Issue and the Editorial
Available online 29 March 2022
https://doi.org/10.1016/j.coelec.2022.100993

Keywords
Transition metal electrocatalysts, Water splitting, CO_2 electroreduction, Oxygen evolution electrocatalyst, Hydrogen evolution electrocatalyst.

Introduction

The family of transition metal chalcogenides has attracted tremendous attention in the materials research community due to its promising future in sensors, energy conversion and energy storage among other applications [1–5]. In addition, transition metal based electrocatalysts for electrochemical energy conversion has attracted significant attention during last several years owing to their high activity, low cost, and facile tunability. Among these electrocatalytic water splitting which includes hydrogen evolution and oxygen evolution reactions (HER and OER, respectively) has been the focus of major research activity [1,6]. The challenge for practical implementation of water splitting technology, however, depends on identification of suitable and stable catalysts, which can lower reaction energy barrier and increase Faraday efficiency for both reactions. Traditionally, Pt metal is most active as HER catalyst, whereas oxides of iridium (Ir), and ruthenium (Ru), exhibit higher OER performance. However, high price and low stability of these precious metal-based catalysts make commercialization difficult. Transition metal-based chalcogenides (TMCs) have recently shown unprecedented high efficiency for HER and OER in wide range of pH. Apart from water splitting, recently TMCs have also shown tremendous success in electrocatalytic CO_2 reduction (CO2RR). Continuous dependence on fossil fuels for several decades had led to accumulation of high levels of CO_2, which has led to several catastrophic environmental effects threatening well-being of mankind. One of the prime objectives of researchers is to develop technologies that can convert CO_2 to useful products thereby closing the carbon loop. Transition metal-based compounds have been specially attractive for such CO_2 utilization technologies, among which the chalcogenides offer special advantage owing to their selectivity towards forming value-added carbon-rich reduction products. [7–11] In this perspective we will highlight recent progress made in transition metal chalcogenides based electrocatalysts for water splitting and CO2RR, and discuss the reasons behind their high activity (Figure 1).

TMC for water splitting

Two major half-reactions, HER and OER, are responsible for total water splitting to create pure H_2 and O_2. Although thermodynamic water splitting voltage is 1.23 V, a much larger potential is required due to energy loss in the electrochemical system necessitating use of suitable electrocatalysts [12]. Several TMCs have recently demonstrated promising performance for HER and OER, surpassing noble metal-based catalysts

Figure 1

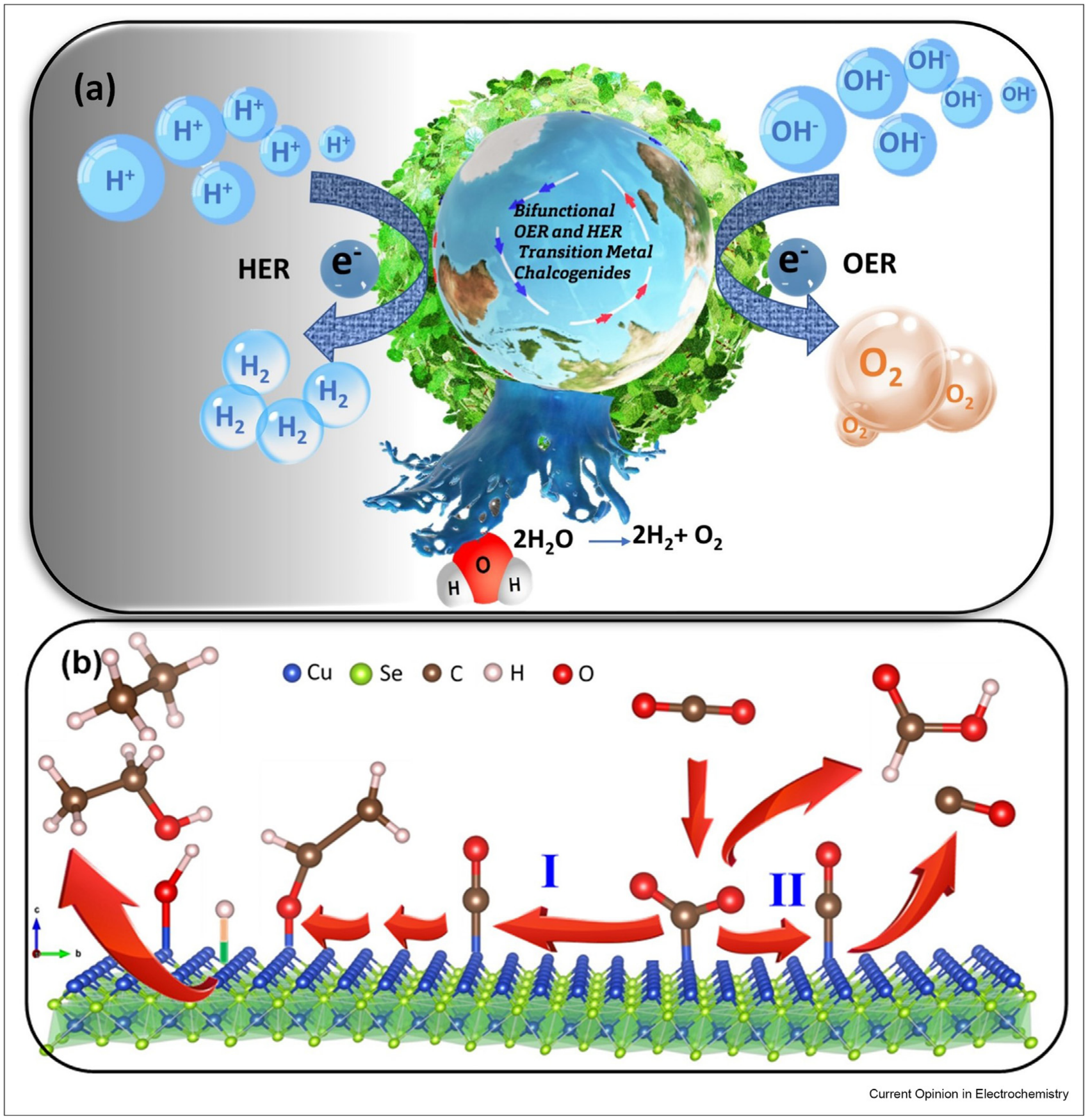

(**a**). Schematic illustration of the TMC electrocatalysts for overall water splitting reaction (HER and OER). (**b**). Schematic representation of CO_2 reduction on catalyst surface proceeding via multi-step electron transfer reaction pathways. The catalyst surface modeled after Cu_2Se also illustrates the importance of catalyst design, whereby increasing intermediate **CO* dwell time on the surface (strong adsorption) can lead to **Pathway I** being more predominant resulting in carbon-rich reduction products. Weak adsorption of **CO* on the other hand leads to predominance of **Pathway II** and ready desorption of CO and HCOOH as products.

[1,13,14]. The TMCs typically exhibit low intrinsic electrical resistivity and rapid charge transfer owing to their electron rich transition metal centers, highly covalent network, and electrochemical tunability. These TMCs are primarily comprised of selenides and tellurides of cobalt, nickel, iron, and copper, in binary and multinary compounds. By modifying the intrinsic and extrinsic structures and compositions of TMCs, a variety of compounds containing different transition metals and chalcogens can be synthesized. In the following sections, binary and multinary (ternary, quaternary, and more complex) chalcogenides have been discussed with respect to electrocatalytic water splitting.

Binary TMCs

Binary metal chalcogenides, more commonly referred to as TMCs, contain one type of transition metal and one type of chalcogen. The most well-known example among them is nickel based binary metal chalcogenides (Ni_xSe_y), which has been widely studied for water splitting. A variety of stoichiometric (Nise, $NiSe_2$, Ni_3Se_2, Ni_3Se_4) and non-stoichiometric ($Ni_{0.85}Se$)

nickel selenides have been investigated for OER and HER [13]. Xu et al., have also compared OER catalytic performance of various Ni-based materials (NiO, NiSe, Ni_3Se_2, and Ni) [15], and have observed that Ni_3Se_2 had the best OER electrocatalytic activity due to the synergistic impact of intrinsic metal states and better surface recombination of anions in metal matrix. Umanga et al. proposed that the major cause for high catalytic activity for Ni-chalcogenides was due to increased covalency of the chalcogenide anions, which increases electrochemical activity of the transition metal center [16]. This hypothesis was confirmed by investigating OER activity of Ni_3Te_2 and comparing it with Ni_3E_2 (E = S, Se, Te) and NiO_x. Ni_3Te_2 showed an overpotential of 180 and 212 mV at 10 mA cm^{-2} for OER and HER, respectively, exhibiting one of the lowest overpotential for OER. This study further confirmed that decreasing electronegativity of the chalcogenide anions [Te (2.1) vs Se (2.55), O (3.44)], led to increased catalytic efficiency attributed to enhanced degree of covalency in nickel tellurides [16]. Figure 2 (a-g) represents the effect of change in chalcogenide anions on OER and HER activity for Ni-based material, which show an order of $Ni_3Te_2 > Ni_3Se_2 > Ni_3S_2$ toward the OER and $NiSe > Ni_3S_2 > Ni_3Te_2$ toward the HER. The effect of electronegativity in improving OER catalytic activity was also confirmed in Co-based composition, whereby, it was observed that $CoTe_2$ showed significantly improved catalytic efficiency compared to Co-oxides and selenide [1]. Density functional theory (DFT) calculations provided further insight into the structure−property correlation of these chalcogenides, wherein the——OH adsorption energy was identified as a key descriptor for OER activity [1]. The tellurides and selenides were observed to exhibit optimal—OH adsorption energy leading to most efficient catalytic activity. Apart from the nickel based chalcogenides, other metal binary metal chalcogenides such as $FeSe_2$ [17], $CoSe_2$ [18], $CoTe_2$ [1], CuSe [19] have aroused interest for bifunctional HER and OER activity.

Multinary TMCs

Since the electron density around the catalytically active transition metal center plays a critical role in defining catalytic activity, it was impervious to tune that electron density through structural and compositional modifications. While changing anions in the chalcogenide series leads to change in lattice electronegativity, doping in the transition metal site can lead to more subtle change in electron density around the catalytic center through d−d transitions and advent of metal−metal bonding. Hence, mixed-transition-metal based electrocatalysts have emerged as new pH-universal electrocatalysts for water-splitting, which has also been characterized by their enhanced electrical conductivity, synergistic impact of bimetallic compositions, and structural stability. Several multinary TMC composites with tunable compositions were investigated in addition to cobalt and nickel chalcogenides. These composites typically outperformed their monometallic counterparts in terms of catalytic performance as has been exemplified through several examples [20,21]. As an example, superior conductivity and reactive properties of Ni−Co bimetallic selenides have been identified as viable electrocatalysts for OER [21]. $NiCoSe_2$@PCM showed outstanding catalytic activity as a bifunctional electrocatalyst, with overpotentials of 116 mV and 140 mV at 10 mA cm^{-2} for HER and OER, respectively [21]. NiFe hybrid selenides have recently been proposed as interesting OER and HER bifunctional catalysts that pave the path for the development of ternary metal chalcogenides. Xianbiao et al. suggested a self-standing $Ni_{0.75}Fe_{0.25}Se_2$@NF electrocatalyst that demonstrated remarkable OER and HER activity with overpotentials of 210 mV and 117 mV, respectively, to achieve current density of 10 mA cm^{-2} [22]. Cao et al. synthesized a bimetallic spinel-structured $CuCo_2Se_4$ electrocatalyst that requires a low overpotential of 320 mV to obtain a current density of 50 mA cm^{-2} for OER and 125 mV to achieve a current density of 10 mA cm^{-2} for HER [6]. Combinatorial electrodeposition was also utilized to examine quaternary mixed metal selenide compositions by exploring the ternary phase diagrams of Ni−Fe−Co, Fe−Cu−Co and Co−Ni−Cu systems as shown in Figure 2(h-j) [23−25]. In this work quaternary composition such as $(Co_{0.21}Ni_{0.25}Cu_{0.54})_3Se_2$, $(Ni_{0.25}Fe_{0.68}Co_{0.07})_3Se_4$ and $(Fe_{0.48}Co_{0.38}Cu_{0.14})Se$ showed the superior OER catalytic performance with overpotential of 272 mV, 230 mV and 256 mV, respectively [Figure 2(h-j)] [23−25]. These experiments demonstrated that transition metal doping enhanced the number of actual catalytically active sites and expedited the rate-determining steps by manipulating the OH-adsorption kinetics on the catalyst surface by changing the local electron density surrounding the catalytic site [26]. Further, Leiming et al. synthesized mixed metal telluride $NiCo_2Te_4$/PTCDA, which showed the superior activity in both OER and HER in neutral pH with overpotential of 120 and 60 mV, respectively. Effect of doping of different transition metals such as Co, Cu, and V into NiSe matrix for water splitting activity was recently demonstrated by Xiaoqiang et al. [27] The catalytic performance of these M−NiSe/NF materials is M-dependent, and it follows the order V−NiSe > Co−NiSe > Cu−NiSe > NiSe toward the OER and Cu−NiSe > Co−NiSe > NiSe > V−NiSe toward the HER. Doping of NiSe with different transition metals is an example of intrinsic effect. An intrinsic doping consisting of doping in the transition metal site, leads to scrambling of the active sites and modulation of electron density around the active site leading to change in catalytic activity [23]. Although this review is focused on alkaline water electrolysis, it must be noted that water splitting has also been conducted in acidic electrolyte to be more compatible with fuel cell systems. Accordingly electrocatalysts for acid water electrolysis has received substantial attention because of its high reaction

Figure 2

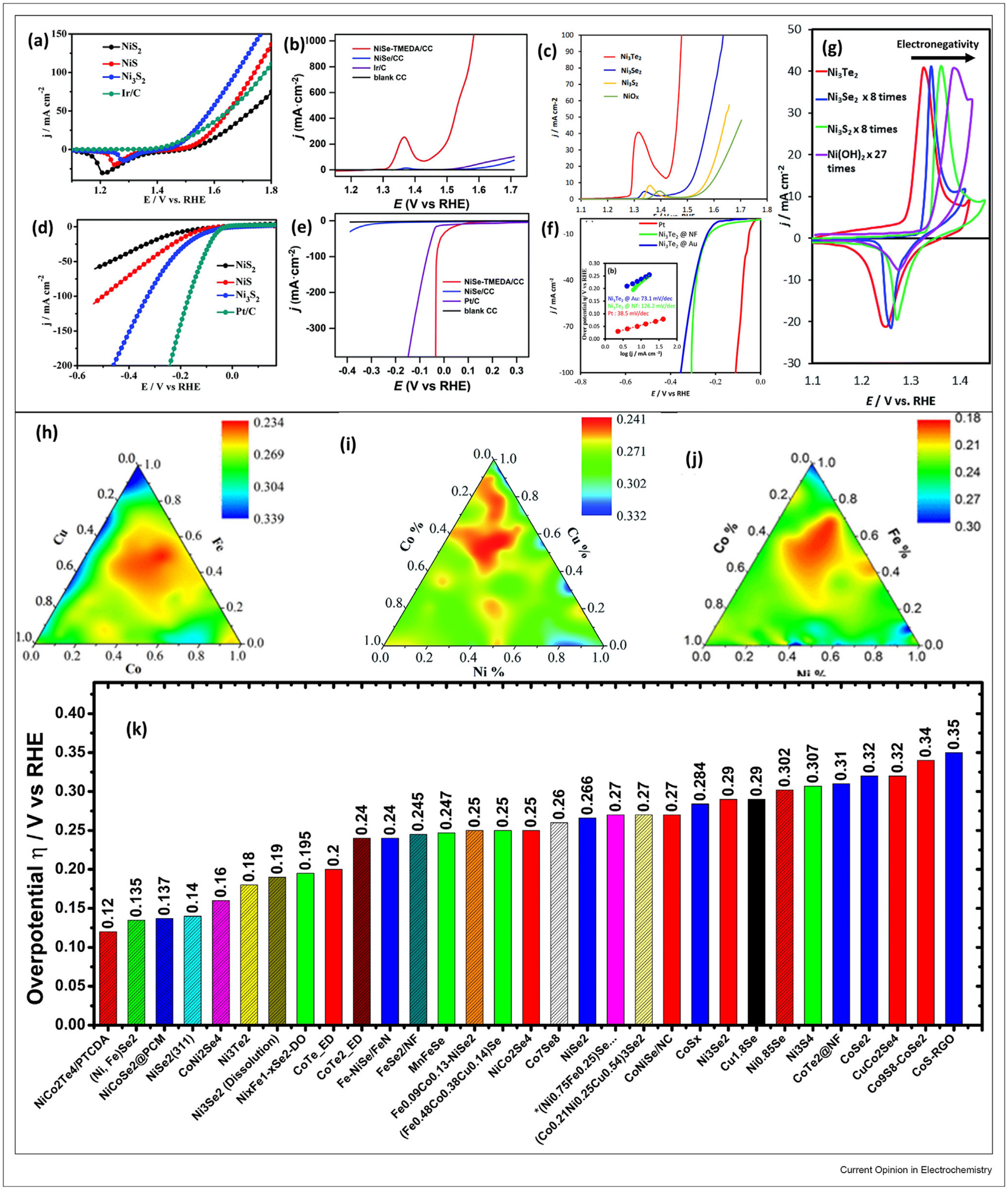

OER and HER polarization curves of (**a, d**) Nickel sulphide [69], (**b, e**) Nickel selenide, [70]. (**c**) Comparison of OER polarization curves for NiO_X, Ni_3S_2, Ni_3Se_2, and Ni_3Te_2 in 1.0 M KOH depicting effect of anion electronegativity on OER activity [16]. (**f**) HER polarization curves of Ni_3Te_2 in 1.0 M KOH. (**g**) Comparison of $Ni^{2+} \rightarrow Ni^{3+}$ oxidation peaks in Ni_3Te_2, Ni3Se2, Ni_3S_2, and $Ni(OH)_2$ confirming effect of anion electronegativity on active site generation [16]. (**h,i,j**) Contour plots of overpotential η (in units of V) at the 10 mA cm^2 for the Fe−Cu−Co, Co−Ni−Cu, Ni−Fe−Co trigonal phase space, respectively [23−25]. (**k**) Comparison of OER activity of various metal chalcogenides at current density of 10 mA cm^{-2} [1,6,36,37,40,42−45,50,51,71,16,72−79,17,20,21,23−25,35]. Adapted with permission from ref. [16,69,70].

efficiency, high current density, low overpotential, and compact design [28–30]. However, the functional and compositional instability of the chalcogenide based electrocatalysts in acidic medium over extended period of time limits their practical application. The overpotentials of the various metal chalcogenide catalysts with high OER activity reported by different research groups has been benchmarked in terms of the overpotential at 10 mA cm^{-2} and shown in Figure 2(k). Analysis of this benchmarking figure confirms certain trends: (i) decreasing electronegativity in the chalcogenide series leads to decreasing overpotential with tellurides forming the most efficient OER electrocatalysts; (ii) transition metal doping enhances electrocatalytic activity for OER making ternary and quaternary chalcogenides as better catalysts than the binaries in the same series. However, for such aliovalent substitution, doping with transition metals with fewer *d*-electrons is found to be more beneficial. This outlook can now be applied for better catalyst design incorporating less electronegative anions along with aliovalent substitution in the catalytically active site. Table 1 represents the progress in binary and multinary metal chalcogenides as bifunctional electrocatalysts for overall water splitting.

Transition metal chalcogenides for CO_2 electroreduction

Research on electrocatalytic conversion of CO_2 has evolved over past few years with respect to developing catalyst composition with special emphasis on achieving selectivity for the reduction products [7–11]. In the following section we will discuss first about Cu and other transition metal-based catalyst and then focus on transition metal chalcogenides. We will highlight new CO2RR catalysts, which will provide fundamental understanding of catalytic processes to achieve product selectivity, that can be helpful for development of efficient CO2RR catalysts in future. From early on transition-based electrocatalysts have been proved as efficient candidates for CO2RR in commercial devices [80]. They have the ability to convert CO_2 into variety of hydrocarbons with good faradaic efficiency. While CO_2 conversion is of utmost importance to reduce atmospheric levels of this greenhouse gas, production of carbon monoxide, i.e., CO as the reduction product does not really mitigate the problem, since CO itself is a toxic gas. The produced CO, hence, needs to be further processed to other carbonaceous product with higher value. Ongoing research is based on improving selectivity for value-added carbon-rich products. It was hypothesized that adsorption energy of intermediate $*CO$ on the transition metal site played a critical role in influencing product composition and selectivity [7]. Specifically, catalysts with smaller adsorption $*CO$ adsorption energy led to preferential formation of CO and formic acid as the reduction product (Figure 3(a)). Catalysts with significantly larger $*CO$ adsorption energy, on the other hand, exhibited surface poisoning with CO. Hence, recent efforts have been guided towards designing catalyst compositions that will have $*CO$ adsorption energy in the moderate range as shown in Figure 3(a). Since metal-to-ligand back bonding plays a major role in deciding binding of intermediate $*CO$ to the transition metal site, optimizing $*CO$ adsorption energy has been attempted by modulating *d*-electron density near the transition metal site through investigating different transition metals and changing anion coordination. The following sections compile various CO2RR catalysts that has been reported based on their *d*-electron density, and also highlights the correlation of $*CO$ adsorption energy with product selectivity as has been studied in chalcogenide-based catalysts.

Copper and other transition metal catalysts

Copper was found to have enhanced activity towards CO2RR producing at least 16 different C1–C3 hydrocarbon/oxygenate products, which is better than other metals but the selectivity was not attained towards a specific product [81]. Other transition metals such as Au [82–86], Ag [81,87,88], Pd [89], Co [11,90], Zn [11,91,92], led to formation of CO as the major product of CO_2 reduction. Similarly, other metal catalysts such as Pb [93], In [94], Sn [89,95], and Bi [96,97], also led to formation of CO predominantly. Polycrystalline Ag is known for producing CO with Faradaic efficiency (FE) of 22.4% at $-0.8\ V_{RHE}$ [11]. DFT based studies revealed that most of these metal catalysts had a weak binding energy towards CO, which led to weaker adsorption and formation of CO as major product. Therefore, there was a need to modify transition metals such as Cu and other metals to get better selectivity for C2+ products.

Transition metal chalcogenides

Copper chalcogenides and other transition metals with d^5-d^{10} *electrons*

It has been proposed that chalcogenide anions increased lattice covalency owing to their decreased electronegativity, which led to enrichment of *d*-electron density near the transition metal site [16]. Hence, it was expected that chalcogenides will show better $*CO$ adsorption energy leading to better selectivity of C2 products [7,91,98]. Indeed DFT calculation revealed that Cu-selenides showed better $*CO$ adsorption energy compared to the base metal and its oxide as shown in Figure 3(a). Experimental studies also confirm that chalcogens favor the formation of C2 products and deter the formation of C1 products because of decrease in surface concentration of CO [11,91]. Investigation of various Cu-based catalysts such as Cu, Cu-oxide, Cu-sulfide and Cu-selenide catalysts, revealed that selectivity towards certain carbon products increased with Cu-chalcogenides compared to Cu. This fact can be

Table 1

The comparison of OER and HER overpotentials with overall water splitting performance of selected bifunctional nonnoble transition binary and multinary metal chalcogenides

Binary TMC'S	Electrolytes	OER_η @ 10 mA cm^{-2} (mV *vs* RHE)	HER_η @ 10 mA cm^{-2} (mV *vs* RHE)	Overall voltage@ 10 mA cm^{-1} (V)	Reference
$FeSe_2$/NF	1 M KOH	245	178	1.73	[17]
p-$CoSe_2$/CC	1M KOH	243	138	1.62	[18]
$CoTe_2$-ED	1M KOH	240	350	–	[1]
CuSe/NF	1M KOH	297	162	1.68	[19]
Ni_3Te_2	1M KOH	180	212	1.66	[16]
CoTe−NF	1M KOH	241	90	1.45	[31]
Ni_3S_2	1M KOH	400	306	2.0	[32]
$Ni_{0.85}Se$/RGO	1M KOH	320 @30 mA cm^{-2}	169	1.64	[33]
$CoSe_2$-NC	1M KOH	360	234	1.47@20 mA cm^{-2}	[34]
$Ni_{0.85}Se$	1M NaOH	302	200	1.73	[35]
$NiSe_2$	1M KOH	266	132	1.547	[36]
$CoTe_2$@NF	1M KOH	310	111	1.605	[37]
$Co_{0.85}Se$	1M KOH	232	129	1.60	[38]
$NiSe_2$/Ni	1M KOH	235	166	1.64	[39]
$CoSe_2$	OER_1M KOH HER_0.5 M H_2SO_4	325	167	–	[40]
$NiS_{0.5}Se_{0.5}$	1M KOH	257	70	1.55	[41]
Co_9S_8−$CoSe_2$	OER_1M KOH HER_0.5 M H_2SO_4	340	61	1.66	[42]
CoSx	1M KOH	284	102	1.64	[43]
CoS-RGO	1M KOH	350	111	1.77	[44]
Multinary TMC'S	**Electrolytes**	**OER_η @ 10 mA cm^{-2} (mV *vs* RHE)**	**HER_η @ 10 mA cm^{-2} (mV *vs* RHE)**	**Overall Voltage@ 10mAcm^{-1} (V)**	**Reference**
$NiCoSe_2$@PCM	OER_1M KOH HER_0.5 M H_2SO_4	137	116	1.73	[21]
$Ni_{0.75}Fe_{0.25}Se_2$@NF	1M KOH	210	117	1.61	[22]
$CuCo_2Se_4$	1M KOH	350@50 mA cm^{-2}	125	1.782 V@50 mA cm^{-2}	[6]
$NiCo_2Te_4$/PTCDA	1 M PBS	120	60	1.55	[20]
$NiCo_2Se_4$	1M KOH	245	122	1.58	[45]
CoNiSe/NC	1M KOH	270	100	1.65	[45]
CoFe−Se−P	OER_0.1M KOH HER_0.5 M H_2SO_4	210	172.5	1.59	[46]
$NiCoSe_{2-x}$/NC	1M KOH	215	89	1.53	[47]
MnCoSe	1M KOH	243	60	1.66@50 mA cm^{-2}	[48]
FeNiSSe	OER_1M KOH HER_1 M H_2SO_4	213	91.2	1.56	[49]
(Ni, Fe)Se_2	1M KOH	135	145	1.58	[50]
$Fe_{0.09}Co_{0.13}$-$NiSe_2$	1M KOH	251	92	1.52	[51]
Mo−$CoSe_2$ NS@NF	1M KOH	234	89	1.54	[52]
$ZnCo_2S_4$/NF	1M KOH	278	185	1.66	[53]
$Fe_{0.08}Ni_{0.77}Se/CNT_3$	1M KOH	204	108	1.53	[54]
P-$(Ni,Fe)_3S_2$/NF	1M KOH	196	98	1.54	[55]
$FeCo_2S_4$−$NiCo_2S_4$/Ti	1M KOH	230	150	1.51	[56]
Fe−MoS_2/NF	OER_1M KOH HER_0.5 M H_2SO_4	230@20 mA cm^{-2}	153	1.52	[57]
H−Fe−CoMoS	1M KOH	282	137	1.6@20 mA cm^{-2}	[58]
GO/Cu_2ZnSnS_4	OER_1M KOH HER_0.5 M H_2SO_4	130	47	–	[59]
Cr-$CoxS_8$		313@100 mA cm^{-2}	120	1.45	[60]
Ni−Fe−S	1M KOH	292	140	1.46	[61]
$CoNiSe_2$/NF	1M KOH	370	170	1.591	[62]
CDs/NiCo2S_4/Ni3S_2/NF	1M KOH	116	127	1.5	[63]
$CuCo_2S_4$	1M KOH	310@100 mA cm^{-2}	65	1.65@20 mA cm^{-2}	[64]
$FeCo_2S_4$/NF	1M KOH	270@50 mA cm^{-2}	132	1.56	[65]
$(Ni_{0.33}Co_{0.67})S_2$ NWs	OER_1M KOH HER_0.5 M H_2SO_4	295@100 mA cm^{-2}	156@100 mA cm^{-2}	1.57	[66]
$NiCo_2S_4$	1M KOH	200@40 mA cm^{-2}	190	1.57	[67]
NCT-$NiCo_2S_4$	1M KOH	330@100 mA cm^{-2}	295@100 mA cm^{-2}	1.6	[68]

Figure 3

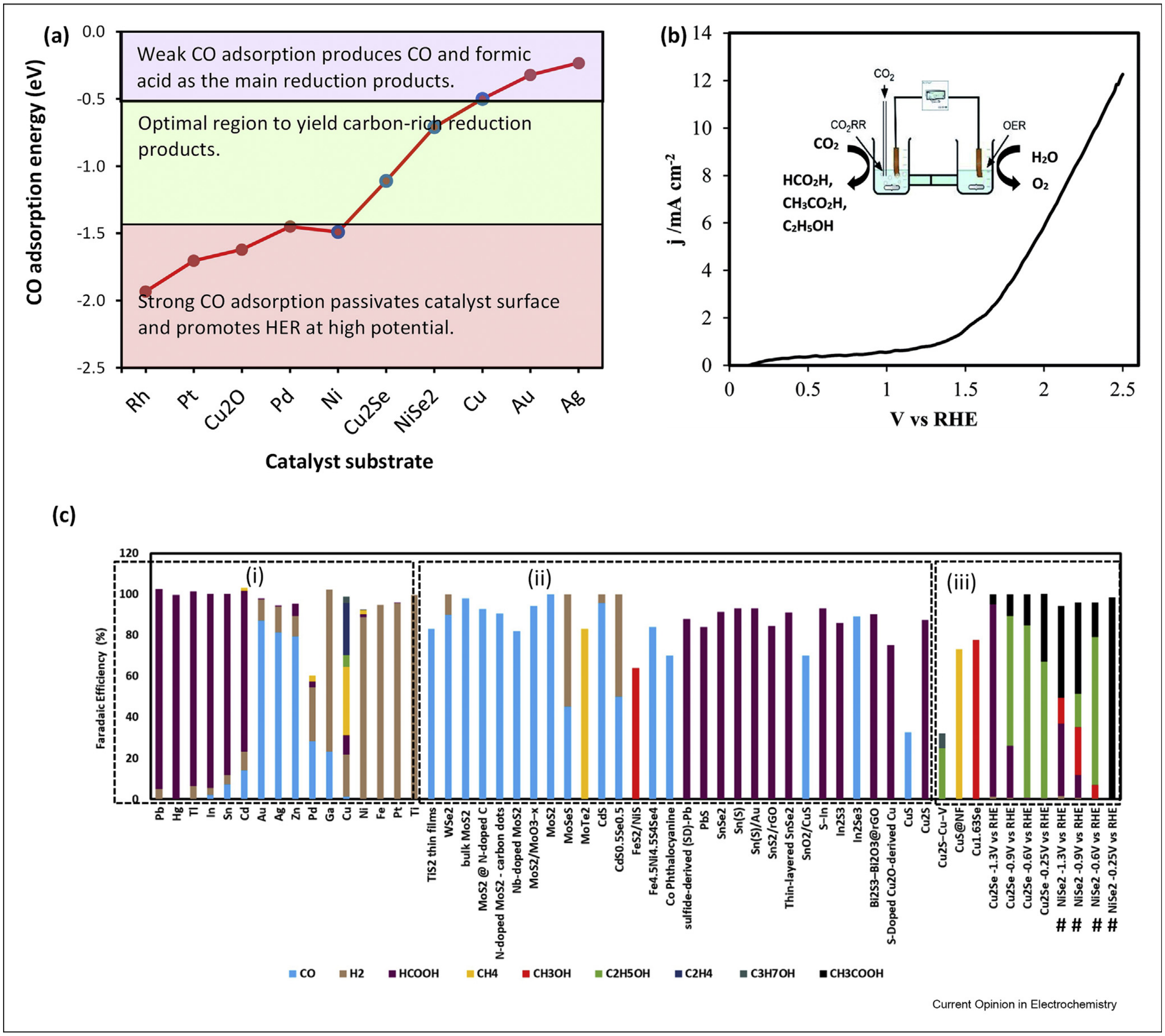

(**a**) Comparison of the *CO adsorption energy calculated on various catalyst surfaces estimated from DFT calculations. (**b**) Experimental setup for comprehensive CO2RR-OER electrochemical cell comprising cathodic CO_2RR and anodic OER with Cu_2Se as both the cathodic and the anodic electrocatalyst. (**c**) Benchmarking of CO2RR activity of various metal chalcogenide electrocatalysts highlighting the various reduction products formed, [8,11, 82, 101,102,116,118–124]. # $NiSe_2$ data has been taken from Saxena et al. unpublished result.

proven by comparing polycrystalline Cu [91,99], and CuS having HCOOH product with FE = 80% at −0.8 V_{RHE} [91], 3D- Cu_2S showing improved performance with a FE = 87.3% at −0.9 V_{RHE} [100], while, Cu_2Se nanocubes [7], and $Cu_{1.63}Se$ nanowires [101], $Cu_{1.8}Se$ nanowires [11], showed a high C2 product selectivity. In case of other transition metals also chalcogenides showed improved activity and selectivity.

FeS_2/NiS showed very good performance in reduction of CO_2 to form CH_3OH with overpotential of 280 mV and Faradaic efficiency of 64% [102]. Using molecular engineering, iron porphyrin was synthesized, which showed good activity achieving 98% Faradaic efficiency for CO production [11]. Cobalt Phthalocyanine with pyridyl moieties as axial ligands achieved 70% FE towards CO production [82]. This study showed that upon axial co-ordination to CoPc, catalytic activity towards CO2RR improved due to energy level rise of d_z^2 orbital [103]. When Ag was modified by sulfur to form Ag_2S, selectivity improved to 92.0% at very low overpotential (−0.754 V) [82,104]. Zn has shown limited activity towards CO2RR

[105]. Zn nanosheets exhibit Faradaic efficiency of 70.9% when producing CO from CO_2 electrochemical reduction. Upon modification with sulfur to make ZnS/Zn, the FE increased to 94.2% [106]. ZnTe is also an efficient catalyst to photochemically convert CO_2 [107]. Similarly Cd also changes selectivity from formic acid to CO when it is converted to CdS [74]. CdS showed good stability of 40+ hours and 95% FE towards CO during CO2RR [11]. Sn is also known to be an active metal towards CO2RR often modulated by surface structure. Modifications such as change in particle size [108], oxide layer thickness [109], morphology [110], and electrolyte's pH have improved the activity, selectivity, energetic efficiency, and robustness of Sn-based catalysts [111,112]. As reported in the study, tin oxide (SnO_x) layer was found to be active because $CO_2^{\bullet}$ intermediate adheres better to the catalyst surface, and oxide layer suppresses the competing hydrogen evolution reaction [113,114]. The catalytic efficiency was improved further by converting SnO_x to $SnSe_2$, which balances the binding strength of $CO_2^{\bullet}$ intermediates and also improves conductivity as compared to oxide layer [115]. The electronic conductivity of metal selenides was found to be better due to higher electronegativity of oxygen than selenium. This also leads to the fast charge transfer during catalytic activity [115]. Hence, $SnSe_2$ showed high current density (12.0 mA cm^{-2}) and high FE (88.4%) at very low potential (−0.76 V vs RHE) for CO2RR [115].

Transition metal with d^1-d^3 *electrons*

Liu et al. showed that ultrathin $MoTe_2$ layers can reduce CO_2 to CH_4 with faradaic efficiency of 83% with extended stability of 45 h. Ultrathin layers lead to highly efficient mass transport due to layered structure, which makes active sites available and improves CO_2 electrochemical reduction [116]. To improve conductivity and number of active sites two-dimensional (2D) $MoSe_2$ doped with transition metals (Fe, Co, Ni, and Cu) were explored using density functional theory (DFT) calculations. Cu doped $MoSe_2$ was found to potentially have great activity for methane production [117]. WSe_2 nanoflakes show activity towards CO2RR at very low overpotential of 0.054 V forming CO as main product (FE = 24%) [82].

Perspective and future outlook

Transition metal chalcogenides have gained considerable attraction in the last few years as electrocatalysts for various electrochemical energy conversion processes owing to their tunable electrochemical properties, structural richness, enhanced charge transfer ability, and possibility of tuning electron density at the catalytic center through doing and vacancy ordering. In this review we have highlighted their high activity for electrocatalytic water splitting and CO_2 electroreduction. Various binary and multinary metal chalcogenides catalysts have been reported for OER with significantly improved catalytic performance compared to the state-of-the-art precious metal-based oxides as shown in Figure 2k. In particular, these catalysts exhibited low η_{10} overpotentials primarily due to facile catalyst activation through enhanced electrochemical tunability of the transition metal center, which is facilitated by the lower electronegativity and higher covalency of the chalcogenide anions. These semiconducting TMCs also have a high potential for use in solar water splitting due to their ideal band gap and acceptable band-edge positions that align well with both water reduction and oxidation potentials. Transition metal dichalcogenides (TMDCs) were previously investigated as potential candidates for photoelectrodes with efficiencies of up to 17% when illuminated in acidic solutions utilizing n-type single crystals [28–30]. Coupling these transition metal chalcogenide electrocatalysts with efficient photo-absorbers to create a hybrid module will lead to significant advances in solar water splitting, by combining low overpotential and functional stability of the electrocatalysts with efficient solar energy capture.

Interestingly, the transition metal chalcogenides function as highly efficient electrocatalysts for CO_2 electroreduction, producing carbon-rich products with high selectivity. Such capability makes these TMC highly applicable for CO_2 utilization, which has become an issue of prime interest to reduce carbon footprint of industrial processes. In this review, we have discussed the fundamental issues related to formation of carbon-rich product from CO_2 electroreduction and its relationship with the underlying chemical reactions on the catalyst surface. By comparing the product formation on various catalyst surfaces it was observed that *CO dwell time on the surface can be used as an appropriate descriptor for tuning the product composition. The *CO dwell time depends on the CO adsorption energy on the catalytic site. Comparison of the CO adsorption energy on various catalyst surfaces showed that weak adsorption energy (leading to less *CO dwell time) resulted in C1 products, whereas very high adsorption energy leads to indefinite stay of *CO on the surface and catalyst poisoning as seen in Ni, Pd, and Pt. This observation offers insight into designing an optimal catalyst surface where the CO adsorption energy should be in the middle range as shown in Figure 3(a) to yield predominantly C2+ products. Tuning anion electronegativity and changing the transition metal center can lead to such optimal *CO adsorption energy as is shown in the benchmark Figure 3(c). The section marked as (i) and (ii) in Figure 3(c) shows catalysts producing mainly C1 products and H_2, wherein, (i) represents the base metals, while (ii) contains the binary and ternary compounds. This can be attributed to lower *CO adsorption energy. Section (iii) represents catalysts that can produce C2+ products. Hence, future outlook for effective CO_2 reduction electrocatalysts with high selectivity for carbon-rich product involves designing the catalyst surface that can facilitate metal—ligand (CO) back-bonding by aligning the metal *d*-orbitals with the ligand (CO) π* orbitals, leading to better CO dwell time on the surface and optimal *CO adsorption energy. Such catalysts can have significant effect on CO_2 utilization by forming value-added chemicals and fuels from waste CO_2.

Several of these TMCs have shown efficient catalytic activity for both anodic and cathodic processes such as OER-HER and OER-CO2RR, respectively, making them suitable as bifunctional electrocatalyst. Among these, the OER-CO2RR bifunctional activity is useful, since such electrocatalytic cell (as shown in Figure 3 (b)), can essentially reduce atmospheric CO_2 to value-added carbon-rich products while enriching O_2 in the atmosphere [7]. Such electrochemical setup has also been used to carry out more economical oxidation processes such as methanol oxidation, ethanol oxidation, urea oxidation etc. [125,126] It will be interesting to explore such electrocatalytic activity for TMCs. Such bifunctional activity can be lucrative for practical industrial applications since it has minimum energy expense and the total cell potential for this methanol oxidation/OER-CO2RR electrolytic cell is lower than combination of individual processes.

Author contributions

Manashi Nath — project conceptualization, funding acquisition, manuscript writing, project administration, supervision; Harish Singh — data acquisition, project execution, manuscript writing, figure, and plot preparation; Apurv Saxena — data acquisition, project execution, manuscript writing, figure, and plot preparation. Harish Singh and Apurv Saxena contributed equally to this manuscript.

Declaration of competing interest

The authors declare that they have no known competing financial interests or personal relationships that could have appeared to influence the work reported in this paper.

References

Papers of particular interest, published within the period of review, have been highlighted as:

* of special interest
** of outstanding interest

1. ** Nath M, De Silva U, Singh H, Perkins M, Liyanage WPR, Umapathi S, Chakravarty S, Masud J: **Cobalt telluride: a highly efficient trifunctional electrocatalyst for water splitting and oxygen reduction**. *ACS Appl Energy Mater* 2021:1c01438, https://doi.org/10.1021/ACSAEM.1C01438. acsaem.

In an alkaline medium, cobalt telluride has been discovered to be an efficient multifunctional electrocatalyst for oxygen and hydrogen evolution reactions as well as oxygen reduction reactions. Electrodeposited CoTe demonstrated the best electrocatalytic activity for OER, requiring an overpotential of 200 mV at 10 mA cm^{-2}. It was observed that –OH adsorption energy on the catalytic site estimated through DFT calculations, can be used as a major descriptor for OER catalytic activity.

2. Singh H, Bernabe J, Chern J, Nath M: **Copper selenide as multifunctional non-enzymatic glucose and dopamine sensor**. *J Mater Res* 2021, **36**:1413–1424, https://doi.org/10.1557/s43578-021-00227-0.

3. Umapathi S, Singh H, Masud J, Nath M: **Nanostructured copper selenide as an ultrasensitive and selective non - enzymatic glucose sensor**. *Mater Adv* 2020, https://doi.org/10.1039/D0MA00890G.

4. Amin BG, Masud J, Nath M: **Facile one-pot synthesis of $NiCo_2Se_4$-rGO on Ni foam for high performance hybrid supercapacitors**. *RSC Adv* 2019, **9**:37939–37946, https://doi.org/10.1039/c9ra06439g.

5. Masud J, Liyanage WPR, Cao X, Saxena A, Nath M: **Copper selenides as high-efficiency electrocatalysts for oxygen evolution reaction**. *ACS Appl Energy Mater* 2018, **1**: 4075–4083, https://doi.org/10.1021/acsaem.8b00746.

6. Cao X, Medvedeva JE, Nath M: **Copper cobalt selenide as a high-efficiency bifunctional electrocatalyst for overall water splitting: combined experimental and theoretical study**. *ACS Appl Energy Mater* 2020, **3**:3092–3103, https://doi.org/10.1021/ACSAEM.0C00262/SUPPL_FILE/AE0C00262_SI_001.PDF.

7. ** Saxena A, Liyanage W, Masud J, Kapila S, Nath M: **Selective electroreduction of CO2 to carbon-rich products with a simple binary copper selenide electrocatalyst**. *J Mater Chem A* 2021, **9**:7150–7161, https://doi.org/10.1039/D0TA11518E.

In this article copper selenide nanocubes have shown high efficiency electrocatalysts for carbon dioxide reduction under ambient conditions. High selectivity for carbon-rich C2 products at a low applied potentials and for C1 products at high potentials was observed. CO adsorption energy on the catalyst surface was proposed to be a critical component in CO_2 reduction on the surface. Cu_2Se surface was studied using experimental and DFT studies for CO_2 reduction.

8. Wang G, Chen J, Ding Y, Cai P, Yi L, Li Y, Tu C, Hou Y, Wen Z, Dai L: **Electrocatalysis for CO_2 conversion: from fundamentals to value-added products**. *Chem Soc Rev* 2021, **50**: 4993–5061, https://doi.org/10.1039/D0CS00071J.

9. Zhu C, Gao D, Ding J, Chao D, Wang J: **TMD-based highly efficient electrocatalysts developed by combined computational and experimental approaches**. *Chem Soc Rev* 2018, **47**: 4332–4356, https://doi.org/10.1039/C7CS00705A.

10. Xie H, Wang T, Liang J, Li Q, Sun S: **Cu-based nanocatalysts for electrochemical reduction of CO2**. *Nano Today* 2018, **21**: 41–54, https://doi.org/10.1016/J.NANTOD.2018.05.001.

11. Shao X, Zhang X, Liu Y, Qiao J, Zhou XD, Xu N, Malcombe JL, Yi J, Zhang J: **Metal chalcogenide-associated catalysts enabling CO_2 electroreduction to produce low-carbon fuels for energy storage and emission reduction: catalyst structure, morphology, performance, and mechanism**. *J Mater Chem A* 2021, **9**:2526–2559, https://doi.org/10.1039/D0TA09232K.

12. Kang Z, Guo H, Wu J, Sun X, Zhang Z, Liao Q, Zhang S, Si H, Wu P, Wang L, Zhang Y, Kang Z, Guo H, Wu J, Sun X, Zhang Z, Liao Q, Zhang S, Si H, Wu P, Zhang Y, Wang L: **Engineering an earth-abundant element-based bifunctional electrocatalyst for highly efficient and durable overall water splitting**. *Adv Funct Mater* 2019, **29**:1807031, https://doi.org/10.1002/ADFM.201807031.

13. Bhat KS, Nagaraja HS: *Recent trends and insights in nickel chalcogenide nanostructures for water-splitting reactions*, **25**; 2019:29–52, https://doi.org/10.1080/14328917.2019.1703523.

14. Singh H, Marley-Hines M, Chakravarty S, Nath M: **Multi-walled carbon nanotube supported manganese selenide as highly active bifunctional OER and ORR electrocatalyst**. *J Mater Chem A* 2022, **6**:4883–5230, https://doi.org/10.1039/D1TA09864K.

15. Xu K, Ding H, Lv H, Tao S, Chen P, Wu X, Chu W, Wu C, Xie Y: **Understanding structure-dependent catalytic performance of nickel selenides for electrochemical water oxidation**. *ACS Catal* 2017, **7**:310–315, https://doi.org/10.1021/ACSCATAL.6B02884/SUPPL_FILE/CS6B02884_SI_001.PDF.

16. ** De Silva U, Masud J, Zhang N, Hong Y, Liyanage WPR, Asle Zaeem M, Nath M: **Nickel telluride as a bifunctional**

electrocatalyst for efficient water splitting in alkaline medium. *J Mater Chem A* 2018, **6**:7608–7622, https://doi.org/10.1039/c8ta01760c.
In this paper, researchers investigate nickel telluride, Ni_3Te_2, as a catalyst for the first time, in order to broaden the family of transition metal chalcogenide-based highly effective OER electrocatalysts. At 10 mA cm^{-2} (180 mV), Ni_3Te_2 electrodeposited on a GC electrode demonstrated the lowest onset potential and overpotential in a series of chalcogenides with identical stoichiometry, Ni_3E_2 (E = S, Se, Te), as well as Ni-oxides.

17. Panda C, Menezes PW, Walter C, Yao S, Miehlich ME, Gutkin V, Meyer K, Driess M: **From a molecular 2Fe-2Se precursor to a highly efficient iron diselenide electrocatalyst for overall water splitting**. *Angew Chem Int Ed* 2017, **56**:10506–10510, https://doi.org/10.1002/ANIE.201706196.

18. Wan S, Jin W, Guo X, Mao J, Zheng L, Zhao J, Zhang J, Liu H, Tang C: **Self-templating construction of porous $CoSe_2$ nanosheet arrays as efficient bifunctional electrocatalysts for overall water splitting**. *ACS Sustain Chem Eng* 2018, **6**: 15374–15382, https://doi.org/10.1021/ACSSUSCHEMENG.8B03804/SUPPL_FILE/SC8B03804_SI_001.PDF.

19. Chakraborty B, Beltrán-Suito R, Hlukhyy V, Schmidt J, Menezes PW, Driess M: **Crystalline copper selenide as a reliable non-noble electro(pre)catalyst for overall water splitting**. *ChemSusChem* 2020, **13**:3222–3229, https://doi.org/10.1002/CSSC.202000445.

20. * Tao L, Huang M, Guo S, Wang Q, Li M, Xiao X, Cao G, Shao Y, Shen Y, Fu Y, Wang M: **Surface modification of NiCo2Te4 nanoclusters: a highly efficient electrocatalyst for overall water-splitting in neutral solution**. *Appl Catal B Environ* 2019, **254**:424–431, https://doi.org/10.1016/J.APCATB.2019.05.010.
The catalytic activity of $NiCo_2Te_4$ nanoclusters was investigated in this article, and it was discovered that surface modification with perylene-tetracarboxylic-dianhydride can greatly improve total water splitting in neutral solution.

21. Poorahong S, Harding DJ, Keawmorakot S, Siaj M: **Free standing bimetallic nickel cobalt selenide nanosheets as three-dimensional electrocatalyst for water splitting**. *J Electroanal Chem* 2021, **897**:115568, https://doi.org/10.1016/J.JELECHEM.2021.115568.

22. * Hu X, Zhou Q, Cheng P, Su S, Wang X, Gao X, Zhou G, Zhang Z, Liu J: **Nickel-iron selenide polyhedral nanocrystal with optimized surface morphology as a high-performance bifunctional electrocatalyst for overall water splitting**. *Appl Surf Sci* 2019, **488**:326–334, https://doi.org/10.1016/j.apsusc.2019.05.220.
As high-performance bifunctional electrocatalysts, Fe-doped $NiSe_2$ polyhedron nanocrystals grown on Ni foam ($Ni_{0.75}Fe_{0.25}Se_2$@NF) with controlled surface morphology are produced in this study. The optimized polyhedron nanocrystals' surfaces have a high density of catalytic active sites on their surfaces.

23. * Cao X, Hong Y, Zhang N, Chen Q, Masud J, Zaeem MA, Nath M: **Phase exploration and identification of multinary transition-metal selenides as high-efficiency oxygen evolution electrocatalysts through combinatorial electrodeposition**. *ACS Catal* 2018, **8**:8273–8289, https://doi.org/10.1021/ACSCATAL.8B01977/SUPPL_FILE/CS8B01977_SI_001.PDF.
This research gives important information on the effect of systematic doping on transition metal selenide-based electrocatalysts incorporating Ni, Fe, and Co, which can be used to build highly efficient OER electrocatalysts using targeted synthesis.

24. Cao X, Johnson E, Nath M: **Expanding multinary selenide based high-efficiency oxygen evolution electrocatalysts through combinatorial electrodeposition: case study with Fe-Cu-Co selenides**. *ACS Sustain Chem Eng* 2019, **7**:9588–9600, https://doi.org/10.1021/acssuschemeng.9b01095.

25. Cao X, Johnson E, Nath M: **Identifying high-efficiency oxygen evolution electrocatalysts from Co–Ni–Cu based selenides through combinatorial electrodeposition**. *J Mater Chem A* 2019, **7**:9877–9889, https://doi.org/10.1039/C9TA00863B.

26. Cao M, Wang H, Kannan P, Ji S, Wang X, Zhao Q, Linkov V, Wang R: **Highly efficient non-enzymatic glucose sensor based on CuxS hollow nanospheres**. *Appl Surf Sci* 2019, **492**: 407–416, https://doi.org/10.1016/j.apsusc.2019.06.248.

27. ** Du X, Ma G, Zhang X: **Experimental and theoretical understanding on electrochemical activation processes of nickel selenide for excellent water-splitting performance: comparing the electrochemical performances with M-NiSe (M = Co, Cu, and V)**. *ACS Sustain Chem Eng* 2019, **7**: 19257–19267, https://doi.org/10.1021/ACSSUSCHEMENG.9B05514/SUPPL_FILE/SC9B05514_SI_001.PDF.
Using a conventional hydrothermal and selenylation process, distinct transition metals (M = Co, Cu, and V) doped into NiSe (M–NiSe) are synthesized for the first time in this work. When V–NiSe and Cu–NiSe are used as anode and cathode catalysts, a cell voltage of 1.50 V is required to produce a current intensity of 10 mA cm^{-2} for overall water splitting.

28. Bozheyev F, Xi F, Plate P, Dittrich T, Fiechter S, Ellmer K: **Efficient charge transfer at a homogeneously distributed $(NH_4)_2Mo_3S_{13}/WSe_2$ heterojunction for solar hydrogen evolution**. *J Mater Chem A* 2019, **7**:10769–10780, https://doi.org/10.1039/C9TA01220F.

29. Bozheyev F, Rengachari M, Berglund SP, Abou-Ras D, Ellmer K: **Passivation of recombination active PdSex centers in (001)-textured photoactive WSe2 films**. *Mater Sci Semicond Process* 2019, **93**:284–289, https://doi.org/10.1016/J.MSSP.2018.12.020.

30. Bozheyev F, Xi F, Ahmet I, Höhn C, Ellmer K: **Evaluation of Pt, Rh, SnO_2, $(NH_4)_2Mo_3S_{13}$, $BaSO_4$ protection coatings on WSe_2 photocathodes for solar hydrogen evolution**. *Int J Hydrogen Energy* 2020, **45**:19112–19120, https://doi.org/10.1016/J.IJHYDENE.2020.04.251.

31. Nisar L, Sadaqat M, Hassan A, Babar NUA, Shah A, Najam-Ul-Haq M, Ashiq MN, Ehsan MF, Joya KS: **Ultrathin CoTe nanoflakes electrode demonstrating low overpotential for overall water splitting**. *Fuel* 2020, **280**:118666, https://doi.org/10.1016/J.FUEL.2020.118666.

32. Ho TA, Bae C, Nam H, Kim E, Lee SY, Park JH, Shin H: **Metallic Ni_3S_2 films grown by atomic layer deposition as an efficient and stable electrocatalyst for overall water splitting**. *ACS Appl Mater Interfaces* 2018, **10**:12807–12815, https://doi.org/10.1021/ACSAMI.8B00813/SUPPL_FILE/AM8B00813_SI_001.PDF.

33. Liu G, Shuai C, Mo Z, Guo R, Liu N, Niu X, Dong Q, Wang J, Gao Q, Chen Y, Liu W: **The one-pot synthesis of porous $Ni_{0.85}Se$ nanospheres on graphene as an efficient and durable electrocatalyst for overall water splitting**. *New J Chem* 2020, **44**:17313–17322, https://doi.org/10.1039/D0NJ04197A.

34. Lu H, Zhang Y, Huang Y, Zhang C, Liu T: **Reaction packaging $CoSe_2$ nanoparticles in N-doped carbon polyhedra with bifunctionality for overall water splitting**. *ACS Appl Mater Interfaces* 2019, **11**:3372–3381, https://doi.org/10.1021/ACSAMI.8B20184/SUPPL_FILE/AM8B20184_SI_001.PDF.

35. Wu X, He D, Zhang H, Li H, Li Z, Yang B, Lin Z, Lei L, Zhang X: **Ni0.85Se as an efficient non-noble bifunctional electrocatalyst for full water splitting**. *Int J Hydrogen Energy* 2016, **41**: 10688–10694, https://doi.org/10.1016/J.IJHYDENE.2016.05.010.

36. Li H, Chen S, Lin H, Xu X, Yang H, Song L, Wang X: **Nickel diselenide ultrathin nanowires decorated with amorphous nickel oxide nanoparticles for enhanced water splitting electrocatalysis**. *Small* 2017, **13**:1701487, https://doi.org/10.1002/SMLL.201701487.

37. Yin Y, Xu J, Guo W, Wang Z, Du X, Chen C, Zheng Z, Liu D, Qu D, Xie Z, Tang H, Li J: **A single-step fabrication of CoTe2 nanofilm electrode toward efficient overall water splitting**. *Electrochim Acta* 2019, **307**:451–458, https://doi.org/10.1016/J.ELECTACTA.2019.03.213.

38. Wu Z, Li J, Zou Z, Wang X: **Folded nanosheet-like $Co_{0.85}Se$ array for overall water splitting**. *J Solid State Electrochem* 2018, **22**:1785–1794, https://doi.org/10.1007/S10008-018-3885-3/FIGURES/6.

39. Zhang J, Wang Y, Zhang C, Gao H, Lv L, Han L, Zhang Z: **Self-Supported porous $NiSe_2$ nanowrinkles as efficient bifunctional electrocatalysts for overall water splitting**. *ACS Sustain Chem Eng* 2018, **6**:2231–2239, https://doi.org/10.1021/ACSSUSCHEMENG.7B03657/SUPPL_FILE/SC7B03657_SI_001.PDF.

40. Lan K, Li J, Zhu Y, Gong L, Li F, Jiang P, Niu F, Li R: **Morphology engineering of $CoSe_2$ as efficient electrocatalyst for water splitting**. *J Colloid Interface Sci* 2019, **539**:646–653, https://doi.org/10.1016/J.JCIS.2018.12.044.

41. ** Wang Y, Li X, Zhang M, Zhou Y, Rao D, Zhong C, Zhang J, Han X, Hu W, Zhang Y, Zaghib K, Wang Y, Deng Y: **Lattice-strain engineering of homogeneous NiS0.5Se0.5 core–shell nanostructure as a highly efficient and robust electrocatalyst for overall water splitting**. *Adv Mater* 2020, **32**:2000231, https://doi.org/10.1002/ADMA.202000231.

Homogeneous lattice-strained nanosheets@nanorods hybrids have been created and produced using a simple technique in this study. The $NiS_{0.5}Se_{0.5}$ with 2.7 percent lattice strain has excellent activity for HER and OER, with low overpotentials of 70 and 257 mV at 10 mA cm^{-2}, respectively, and excellent long-term durability, even at a high current density of 100 mA cm-2 (300 h), far surpassing other benchmarks and precious metal catalysts.

42. Chakrabartty S, Karmakar S, Raj CR: **An electrocatalytically active nanoflake-like Co_9S_8-$CoSe_2$ Heterostructure for overall water splitting**. *ACS Appl Nano Mater* 2020, **3**:11326–11334, https://doi.org/10.1021/ACSANM.0C02431/SUPPL_FILE/AN0C02431_SI_001.PDF.

43. Bian H, Chen T, Chen Z, Liu J, Li Z, Du P, Zhou B, Zeng X, Tang J, Liu C: **One-step synthesis of mesoporous Cobalt sulfides (CoSx) on the metal substrate as an efficient bifunctional electrode for overall water splitting**. *Electrochim Acta* 2021, **389**:138786, https://doi.org/10.1016/J.ELECTACTA.2021.138786.

44. Chen Y, Xu S, Zhu S, Jiji Jacob R, Pastel G, Wang Y, Li Y, Dai J, Chen F, Xie H, Liu B, Yao Y, Salamanca-Riba LG, Zachariah MR, Li T, Hu L: ***Millisecond synthesis of CoS nanoparticles for highly efficient overall water splitting*** (n.d.), https://doi.org/10.1007/s12274-019-2304-0.

45. Janani G, Yuvaraj S, Surendran S, Chae Y, Sim Y, Song SJ, Park W, Kim MJ, Sim U: **Enhanced bifunctional electrocatalytic activity of Ni-Co bimetallic chalcogenides for efficient water-splitting application**. *J Alloys Compd* 2020, **846**: 156389, https://doi.org/10.1016/J.JALLCOM.2020.156389.

46. He L, Cui B, Hu B, Liu J, Tian K, Wang M, Song Y, Fang S, Zhang Z, Jia Q: **Mesoporous nanostructured CoFe-Se-P composite derived from a prussian blue analogue as a superior electrocatalyst for efficient overall water splitting**. *ACS Appl Energy Mater* 2018, **1**:3915–3928, https://doi.org/10.1021/ACSAEM.8B00663/SUPPL_FILE/AE8B00663_SI_001.PDF.

47. Li J, Wan M, Li T, Zhu H, Zhao Z, Wang Z, Wu W, Du M: **$NiCoSe_2$-x/N-doped C mushroom-like core/shell nanorods on N-doped carbon fiber for efficiently electrocatalyzed overall water splitting**. *Electrochim Acta* 2018, **272**:161–168, https://doi.org/10.1016/J.ELECTACTA.2018.04.032.

48. Mei G, Liang H, Wei B, Shi H, Ming F, Xu X, Wang Z: **Bimetallic MnCo selenide yolk shell structures for efficient overall water splitting**. *Electrochim Acta* 2018, **290**:82–89, https://doi.org/10.1016/J.ELECTACTA.2018.09.062.

49. Majhi KC, Yadav M: **Bimetallic chalcogenide nanocrystallites as efficient electrocatalyst for overall water splitting**. *J Alloys Compd* 2021, **852**:156736, https://doi.org/10.1016/J.JALLCOM.2020.156736.

50. Zhang C, Zhang Y, Zhou S, Li C: **Self-supported iron-doping $NiSe_2$ nanowrinkles as bifunctional electrocatalysts for electrochemical water splitting**. *J Alloys Compd* 2020, **818**: 152833, https://doi.org/10.1016/J.JALLCOM.2019.152833.

51. Sun Y, Xu K, Wei Z, Li H, Zhang T, Li X, Cai W, Ma J, Jin Fan H, Li Y, Sun YQ, Li HL, Zhang T, Li XY, Cai WP, Li Y, Xu K, Fan HJ, Wei ZX, Ma JM: **Strong electronic interaction in dual-cation-incorporated $NiSe_2$ nanosheets with lattice distortion for highly efficient overall water splitting**. *Adv Mater* 2018, **30**: 1802121, https://doi.org/10.1002/ADMA.201802121.

52. Huang J, Wang S, Nie J, Huang C, Zhang X, Wang B, Tang J, Du C, Liu Z, Chen J: **Active site and intermediate modulation of 3D $CoSe_2$ nanosheet array on Ni foam by Mo doping for high-efficiency overall water splitting in alkaline media**. *Chem Eng J* 2021, **417**:128055, https://doi.org/10.1016/J.CEJ.2020.128055.

53. Song G, Wang Z, Sun J, Sun J, Yuan D, Zhang L: **$ZnCo_2S_4$ nanosheet array anchored on nickel foam as electrocatalyst for electrochemical water splitting**. *Electrochem Commun* 2019, **105**:106487, https://doi.org/10.1016/J.ELECOM.2019.106487.

54. Liu G, Shuai C, Mo Z, Guo R, Liu N, Dong Q, Wang J, Pei H, Liu W, Guo X: **Fe-doped Ni0.85Se nanospheres interspersed into carbon nanotubes as efficient and stable electrocatalyst for overall water splitting**. *Electrochim Acta* 2021, **385**:138452, https://doi.org/10.1016/J.ELECTACTA.2021.138452.

55. Liu C, Jia D, Hao Q, Zheng X, Li Y, Tang C, Liu H, Zhang J, Zheng X: **P-doped iron-nickel sulfide nanosheet arrays for highly efficient overall water splitting**. *ACS Appl Mater Interfaces* 2019, **11**:27667–27676, https://doi.org/10.1021/ACSAMI.9B04528/SUPPL_FILE/AM9B04528_SI_002.AVI.

56. Li D, Liu Z, Wang J, Liu B, Qin Y, Yang W, Liu J: **Hierarchical trimetallic sulfide FeCo2S4–NiCo2S4 nanosheet arrays supported on a Ti mesh: an efficient 3D bifunctional electrocatalyst for full water splitting**. *Electrochim Acta* 2020, **340**: 135957, https://doi.org/10.1016/J.ELECTACTA.2020.135957.

57. Xue JY, Li FL, Zhao ZY, Li C, Ni CY, Gu HW, Young DJ, Lang JP: **In situ generation of bifunctional Fe-doped MoS2 nanocanopies for efficient electrocatalytic water splitting**. *Inorg Chem* 2019, **58**:11202–11209, https://doi.org/10.1021/ACS.INORGCHEM.9B01814/SUPPL_FILE/IC9B01814_SI_001.PDF.

58. Guo Y, Zhou X, Tang J, Tanaka S, Kaneti YV, Na J, Jiang B, Yamauchi Y, Bando Y, Sugahara Y: **Multiscale structural optimization: highly efficient hollow iron-doped metal sulfide heterostructures as bifunctional electrocatalysts for water splitting**. *Nano Energy* 2020, **75**:104913, https://doi.org/10.1016/J.NANOEN.2020.104913.

59. * Digraskar RV, Sapner VS, Ghule AV, Sathe BR: *Enhanced overall water-splitting performance: oleylamine-functionalized GO/Cu2ZnSnS4 composite as a nobel metal-free and NonPrecious electrocatalyst.* ACS Omega; 2019, https://doi.org/10.1021/ACSOMEGA.9B01680/SUPPL_FILE/AO9B01680_SI_001.PDF.

In this work, researchers have developed an oleylamine-functionalized graphene oxide/Cu_2ZnSnS_4 composite (OAm-GO/CZTS) and tested it as a higher bifunctional electrocatalyst for HER and OER reactions. With overpotentials of 47 mV for HER and 1.36 V for OER at a current density of 10 mA cm^{-2}, the OAm-GO/CZTS exhibits excellent electrocatalytic activity and endurance toward H_2 and O_2 in both acidic and basic environments.

60. Du X, Su H, Zhang X: **Cr doped-Co_9S_8 nanoarrays as high-efficiency electrocatalysts for water splitting**. *J Alloys Compd* 2020, **824**:153965, https://doi.org/10.1016/J.JALLCOM.2020.153965.

61. Zhang C, Zhou S, Dong X, Han Y, Li J, Yin W: **Three-dimensional self-supported iron-doped nickel sulfides for sustainable overall water splitting**. *Vacuum* 2020, **181**:109661, https://doi.org/10.1016/J.VACUUM.2020.109661.

62. Chen T, Tan Y: **Hierarchical $CoNiSe_2$ nano-architecture as a high-performance electrocatalyst for water splitting**. *Nano Res* 2018, **11**:1331–1344, https://doi.org/10.1007/S12274-017-1748-3. 2018 113.

63. Zhao X, Liu H, Rao Y, Li X, Wang J, Xia G, Wu M: **Carbon dots decorated hierarchical $NiCo_2S_4/Ni_3S_2$ composite for efficient water splitting**. *ACS Sustain Chem Eng* 2019, **7**:2610–2618, https://doi.org/10.1021/ACSSUSCHEMENG.8B05611/SUPPL_FILE/SC8B05611_SI_001.PDF.

64. Czioska S, Wang J, Teng X, Chen Z: **Hierarchically structured CuCo2S4 nanowire arrays as efficient bifunctional electrocatalyst for overall water splitting**. *ACS Sustain Chem Eng* 2018, **6**:11877–11883, https://doi.org/10.1021/ACSSUSCHEMENG.8B02155/SUPPL_FILE/SC8B02155_SI_001.PDF.

65. Hu J, Ou Y, Li Y, Gao D, Zhang Y, Xiao P: **FeCo2S4 nanosheet arrays supported on Ni foam: an efficient and durable bifunctional electrocatalyst for overall water-splitting**. *ACS*

Sustain Chem Eng 2018, **6**:11724–11733, https://doi.org/10.1021/ACSSUSCHEMENG.8B01978/SUPPL_FILE/SC8B01978_SI_001.PDF.

66. Zhang Q, Ye C, Li XL, Deng YH, Tao BX, Xiao W, Li LJ, Li NB, Luo HQ: **Self-interconnected porous networks of NiCo disulfide as efficient bifunctional electrocatalysts for overall water splitting**. *ACS Appl Mater Interfaces* 2018, **10**:27723–27733, https://doi.org/10.1021/ACSAMI.8B04386/SUPPL_FILE/AM8B04386_SI_002.AVI.

67. Du X, Lian W, Zhang X: **Homogeneous core–shell NiCo2S4 nanorods as flexible electrode for overall water splitting**. *Int J Hydrogen Energy* 2018, **43**:20627–20635, https://doi.org/10.1016/J.IJHYDENE.2018.09.123.

68. Li F, Xu R, Li Y, Liang F, Zhang D, Fu WF, Lv XJ: **N-doped carbon coated NiCo2S4 hollow nanotube as bifunctional electrocatalyst for overall water splitting**. *Carbon N Y* 2019, **145**:521–528, https://doi.org/10.1016/J.CARBON.2019.01.065.

69. * Zheng X, Han X, Zhang Y, Wang J, Zhong C, Deng Y, Hu W: **Controllable synthesis of nickel sulfide nanocatalysts and their phase-dependent performance for overall water splitting**. *Nanoscale* 2019, **11**:5646–5654, https://doi.org/10.1039/C8NR09902B.

NiSx (i.e., NiS, Ni_3S_2, and NiS_2) nanocrystals have been synthesized through a simple polyol solution method and their electrocatalytic characteristics toward OER and HER have been thoroughly examined. The electrochemical results show that Ni_3S_2 outperforms NiS and NiS_2 in terms of OER and HER performance, producing 1.63 V to achieve a current density of 10 mA cm^{-2} in the total water splitting device, which is comparable to that of noble metal catalysts.

70. ** Chen D, Chen Y, Zhang W, Cao R: **Nickel selenide from single-molecule electrodeposition for efficient electrocatalytic overall water splitting**. *New J Chem* 2021, **45**:351–357, https://doi.org/10.1039/D0NJ04966B.

As reported in this paper, the performance of the as-prepared electrodes (NiSe-TMEDA/CC) in alkaline solution for water splitting was investigated. The electrodes demonstrated bifunctional OER and HER activity with small overpotentials of 226 and 30.8 mV, respectively, to achieve current densities of 100 mA cm^{-2}.

71. Swesi AT, Masud J, Liyanage WPR, Umapathi S, Bohannan E, Medvedeva J, Nath M: **Textured NiSe2 film: bifunctional electrocatalyst for full water splitting at remarkably low overpotential with high energy efficiency/639/638/77/886/639/301/299/886/639/301/299/161/128/120/145/140/146 article**. *Sci Rep* 2017, **7**:1–11, https://doi.org/10.1038/s41598-017-02285-z.

72. Amin BG, Swesi AT, Masud J, Nath M, Li R, Chemcomm C: **Communication, CoNi 2 Se 4 as an efficient bifunctional electrocatalyst for overall water splitting**. *Chem Commun* 2017, **53**:5412–5415, https://doi.org/10.1039/C7CC01489A.

73. Xu X, Song F, Hu X: *ARTICLE A nickel iron diselenide-derived efficient oxygen-evolution catalyst*. Nat. Publ. Gr.; 2016, https://doi.org/10.1038/ncomms12324.

74. Wang C, Cao M, Jiang X, Wang M, Shen Y: **A catalyst based on copper-cadmium bimetal for electrochemical reduction of CO2 to CO with high faradaic efficiency**. *Electrochim Acta* 2018, **271**:544–550, https://doi.org/10.1016/J.ELECTACTA.2018.03.156.

75. Sun M, Gao R-T, Liu X, Gao R, Wang L: **Manganese-based oxygen evolution catalysts boosting stable solar-driven water splitting: MnSe as an intermetallic phase**. *J Mater Chem A* 2020, **8**:25298–25305, https://doi.org/10.1039/D0TA09946E.

76. Masud J, Nath M: **Co7Se8 nanostructures as catalysts for oxygen reduction reaction with high methanol tolerance**. *ACS Energy Lett* 2016, **1**:27–31, https://doi.org/10.1021/acsenergylett.6b00006.

77. Swesi AT, Masud J, Nath M: **Nickel selenide as a high-efficiency catalyst for oxygen evolution reaction**. *Energy Environ Sci* 2016, **9**:1771–1782, https://doi.org/10.1039/C5EE02463C.

78. Wan K, Luo J, Zhou C, Zhang T, Arbiol J, Lu X, Mao BW, Zhang X, Fransaer J: **Hierarchical porous Ni3S4 with enriched high-valence Ni sites as a robust electrocatalyst for efficient oxygen evolution reaction**. *Adv Funct Mater* 2019, **29**:1900315, https://doi.org/10.1002/ADFM.201900315.

79. Swesi AT, Masud J, Nath M: **Enhancing electrocatalytic activity of bifunctional Ni3Se2 for overall water splitting through etching-induced surface nanostructuring**. *J Mater Res* 2016, **31**:2888–2896, https://doi.org/10.1557/jmr.2016.301.

80. Johnson D, Qiao Z, Djire A: **Progress and challenges of carbon dioxide reduction reaction on transition metal based electrocatalysts**. *ACS Appl Energy Mater* 2021, **4**:8661–8684, https://doi.org/10.1021/ACSAEM.1C01624.

81. Nitopi S, Bertheussen E, Scott SB, Liu X, Engstfeld AK, Horch S, Seger B, Stephens IEL, Chan K, Hahn C, Nørskov JK, Jaramillo TF, Chorkendorff I: **Progress and perspectives of electrochemical CO2 reduction on copper in aqueous electrolyte**. *Chem Rev* 2019, **119**:7610–7672, https://doi.org/10.1021/ACS.CHEMREV.8B00705/SUPPL_FILE/CR8B00705_SI_001.PDF.

82. Gao FY, Wu ZZ, Gao MR: **Electrochemical CO2Reduction on transition-metal chalcogenide catalysts: recent advances and future perspectives**. *Energy Fuel* 2021, **35**:12869–12883, https://doi.org/10.1021/ACS.ENERGYFUELS.1C01650.

83. Zhu W, Zhang YJ, Zhang H, Lv H, Li Q, Michalsky R, Peterson AA, Sun S: **Active and selective conversion of CO2 to CO on ultrathin Au nanowires**. *J Am Chem Soc* 2014, **136**:16132–16135, https://doi.org/10.1021/JA5095099/SUPPL_FILE/JA5095099_SI_001.PDF.

84. Lee HE, Yang KD, Yoon SM, Ahn HY, Lee YY, Chang H, Jeong DH, Lee YS, Kim MY, Nam KT: **Concave rhombic dodecahedral Au nanocatalyst with multiple high-index facets for CO2 reduction**. *ACS Nano* 2015, **9**:8384–8393, https://doi.org/10.1021/ACSNANO.5B03065/SUPPL_FILE/NN5B03065_SI_001.PDF.

85. Chen Y, Li CW, Kanan MW: **Aqueous CO2 reduction at very low overpotential on oxide-derived au nanoparticles**. *J Am Chem Soc* 2012, **134**:19969–19972, https://doi.org/10.1021/JA309317U/SUPPL_FILE/JA309317U_SI_001.PDF.

86. Zhu W, Michalsky R, Metin Ö, Lv H, Guo S, Wright CJ, Sun X, Peterson AA, Sun S: **Monodisperse Au nanoparticles for selective electrocatalytic reduction of CO2 to CO**. *J Am Chem Soc* 2013, **135**:16833–16836, https://doi.org/10.1021/JA409445P/SUPPL_FILE/JA409445P_SI_001.PDF.

87. Ham YS, Choe S, Kim MJ, Lim T, Kim SK, Kim JJ: **Electrodeposited Ag catalysts for the electrochemical reduction of CO2 to CO**. *Appl Catal B Environ* 2017, **208**:35–43, https://doi.org/10.1016/J.APCATB.2017.02.040.

88. Luc W, Collins C, Wang S, Xin H, He K, Kang Y, Jiao F: **Ag-sn bimetallic catalyst with a core-shell structure for CO2 reduction**. *J Am Chem Soc* 2017, **139**:1885–1893, https://doi.org/10.1021/JACS.6B10435/SUPPL_FILE/JA6B10435_SI_001.PDF.

89. Zhang X, Guo SX, Gandionco KA, Bond AM, Zhang J: **Electrocatalytic carbon dioxide reduction: from fundamental principles to catalyst design**. *Mater Today Adv* 2020, **7**:100074, https://doi.org/10.1016/J.MTADV.2020.100074.

90. Abdelwahab A, Castelo-Quibén J, Pérez-Cadenas M, Elmouwahidi A, Maldonado-Hódar FJ, Carrasco-Marín F, Pérez-Cadenas AF: **Cobalt-doped carbon gels as electro-catalysts for the reduction of CO2 to hydrocarbons**. *Catal* 2017, **7**:25–27, https://doi.org/10.3390/CATAL7010025. 25.

91. Zhao J, Xue S, Barber J, Zhou Y, Meng J, Ke X: **An overview of Cu-based heterogeneous electrocatalysts for CO2 reduction**. *J Mater Chem A* 2020, **8**:4700–4734, https://doi.org/10.1039/C9TA11778D.

92. Albo J, Sáez A, Solla-Gullón J, Montiel V, Irabien A: **Production of methanol from CO_2 electroreduction at Cu_2O and Cu_2O/ZnO-based electrodes in aqueous solution**. *Appl Catal B Environ* 2015, **176–177**:709–717, https://doi.org/10.1016/J.APCATB.2015.04.055.

93. Zhao CX, Bu YF, Gao W, Jiang Q: **CO_2 reduction mechanism on the Pb(111) surface: effect of solvent and cations**. *J Phys Chem C* 2017, **121**:19767–19773, https://doi.org/10.1021/ACS.JPCC.7B04375/SUPPL_FILE/JP7B04375_SI_001.PDF.

94. Ye F, Gao J, Chen Y, Fang Y: **Oxidized indium with transformable dimensions for CO2 electroreduction toward**

formate aided by oxygen vacancies. *Sustain Energy Fuels* 2020, **4**:3726–3731, https://doi.org/10.1039/D0SE00498G.

95. Zheng X, De Luna P, García de Arquer FP, Zhang B, Becknell N, Ross MB, Li YY, Banis MN, Li YY, Liu M, Voznyy O, Dinh CT, Zhuang T, Stadler P, Cui Y, Du X, Yang P, Sargent EH, De Luna P, de Arquer FPG, Zhang B, Becknell N, Ross MB, Li YY, Banis MN, Li YY, Liu M, Voznyy O, Dinh CT, Zhuang T, Stadler P, Cui Y, Du X, Yang P, Sargent EH: **Sulfur-modulated tin sites enable highly selective electrochemical reduction of CO2 to formate**. *Joule* 2017, **1**:794–805.

96. Deng P, Wang H, Qi R, Zhu J, Chen S, Yang F, Zhou L, Qi K, Liu H, Xia BY: **Bismuth oxides with enhanced bismuth-oxygen structure for efficient electrochemical reduction of carbon dioxide to formate**. *ACS Catal* 2020, **10**:743–750, https://doi.org/10.1021/ACSCATAL.9B04043/SUPPL_FILE/CS9B04043_SI_001.PDF.

97. Atifi A, Keane TP, Dimeglio JL, Pupillo RC, Mullins DR, Lutterman DA, Rosenthal J: **Insights into the composition and function of a bismuth-based catalyst for reduction of CO2 to CO**. *J Phys Chem C* 2019, **123**:9087–9095, https://doi.org/10.1021/ACS.JPCC.9B00504/SUPPL_FILE/JP9B00504_SI_001.PDF.

98. Calvinho KUD, Alherz AW, Yap KMK, Laursen AB, Hwang S, Bare ZJL, Clifford Z, Musgrave CB, Dismukes GC: **Surface hydrides on Fe2P electrocatalyst reduce CO2 at low overpotential: steering selectivity to ethylene glycol**. *J Am Chem Soc* 2021, **143**:21275–21285, https://doi.org/10.1021/JACS.1C03428.

99. * Yoshio Hori, Katsuhei Kikuchi, Shin Suzuki: *Production of CO and CH4 IN electrochemical reduction OF CO2 at metal electrodes IN aqueous hydrogencarbonate solution*, **14**; 2006:1695–1698, https://doi.org/10.1246/CL.1985.1695.

This was one of the first work on CO_2 electroreduction. In this study, electrochemical reduction of CO_2 at different metal electrodes produced products such as CO, formic acid, methane, ethyne, and alcohols such as ethanol in aqueous media. Metal electrodes were characterized into two groups according to the products, Cu, Au, Ag, Zn, Pd, Ga, Ni, Pt producing CO and Pb, Hg, In, Sn, Cd, Tl yielding formic acid.

100. He W, Liberman I, Rozenberg I, Ifraemov R, Hod I: **Electrochemically driven cation exchange enables the rational design of active CO 2 reduction electrocatalysts**. *Angew Chem* 2020, **132**:8339–8346, https://doi.org/10.1002/ANGE.202000545.

101. Yang D, Zhu Q, Chen C, Liu H, Liu Z, Zhao Z, Zhang X, Liu S, Han B: **Selective electroreduction of carbon dioxide to methanol on copper selenide nanocatalysts**. *Nat Commun* 2019, **10**:1–9, https://doi.org/10.1038/s41467-019-08653-9. 2019 101.

102. Zhao S, Guo S, Zhu C, Gao J, Li H, Huang H, Liu Y, Kang Z: **Achieving electroreduction of CO2 to CH3OH with high selectivity using a pyrite–nickel sulfide nanocomposite**. *RSC Adv* 2017, **7**:1376–1381, https://doi.org/10.1039/C6RA26868D.

103. Zimmerman PM, McCrory CCL, Rivera Cruz KE, Liu Y, Soucy TL: **Increasing the CO2 reduction activity of cobalt phthalocyanine by modulating the σ-donor strength of axially coordinating ligands**. *ACS Catal* 2021, **11**:13203–13216, https://doi.org/10.1021/ACSCATAL.1C02379/SUPPL_FILE/CS1C02379_SI_002.PDF.

104. Zeng L, Shi J, Luo J, Chen H: **Silver sulfide anchored on reduced graphene oxide as a high -performance catalyst for CO2 electroreduction**. *J Power Sources* 2018, **398**:83–90, https://doi.org/10.1016/J.JPOWSOUR.2018.07.049.

105. Hori Y: **Electrochemical CO<Subscript>2</Subscript> reduction on metal electrodes**. *Mod Aspect Electrochem* 2008: 89–189, https://doi.org/10.1007/978-0-387-49489-0_3.

106. Zhen JZ, Liu JX, Chen TY, Shi F, Dai YN, Yang B, Li YF, Wang X, Nong TG, Hu YQ, Shi J: **Fabrication of ZnS/Zn electrode using sulphur infiltration method for CO2 reduction into CO in organic media**. *J Alloys Compd* 2019, **771**:994–999, https://doi.org/10.1016/J.JALLCOM.2018.08.318.

107. Jang J-WW, Cho S, Magesh G, Jang YJ, Kim JY, Kim WY, Seo JK, Kim S, Lee K-HH, Lee JS: **Aqueous-solution route to zinc telluride films for application to CO2 reduction**. *Angew Chem Int Ed* 2014, **53**:5852–5857, https://doi.org/10.1002/ANIE.201310461.

108. Zhang S, Kang P, Meyer TJ: **Nanostructured tin catalysts for selective electrochemical reduction of carbon dioxide to formate**. *J Am Chem Soc* 2014, **136**:1734–1737, https://doi.org/10.1021/JA4113885/SUPPL_FILE/JA4113885_SI_001.PDF.

109. Wu J, Risalvato FG, Ma S, Zhou XD: **Electrochemical reduction of carbon dioxide III. The role of oxide layer thickness on the performance of Sn electrode in a full electrochemical cell**. *J Mater Chem A* 2014, **2**:1647–1651, https://doi.org/10.1039/C3TA13544F.

110. Won DH, Choi CH, Chung J, Chung MW, Kim EH, Woo SI: **Rational design of a hierarchical tin dendrite electrode for efficient electrochemical reduction of CO2**. *ChemSusChem* 2015, **8**:3092–3098, https://doi.org/10.1002/CSSC.201500694.

111. Wu J, Risalvato FG, Ke F-S, Pellechia PJ, Zhou X-D: **Electrochemical reduction of carbon dioxide I. Effects of the electrolyte on the selectivity and activity with Sn electrode**. *J Electrochem Soc* 2012, **159**:F353–F359, https://doi.org/10.1149/2.049207JES/XML.

112. Lv W, Zhang R, Gao P, Lei L: **Studies on the faradaic efficiency for electrochemical reduction of carbon dioxide to formate on tin electrode**. *J Power Sources* 2014, **253**:276–281, https://doi.org/10.1016/J.JPOWSOUR.2013.12.063.

113. Chen Y, Kanan MW: **Tin oxide dependence of the CO 2 reduction efficiency on tin electrodes and enhanced activity for tin/tin oxide thin-film catalysts**. *J Am Chem Soc* 2012, **134**: 1986–1989, https://doi.org/10.1021/JA2108799/SUPPL_FILE/JA2108799_SI_001.PDF.

114. Pander JE, Baruch MF, Bocarsly AB: **Probing the mechanism of aqueous CO2 reduction on post-transition-metal electrodes using ATR-IR spectroelectrochemistry**. *ACS Catal* 2016, **6**:7824–7833, https://doi.org/10.1021/ACSCATAL.6B01879.

115. * He B, Jia L, Cui Y, Zhou W, Sun J, Xu J, Wang Q, Zhao L: **SnSe2 nanorods on carbon Cloth as a highly selective, active, and flexible electrocatalyst for electrochemical reduction of CO2 into formate**. *ACS Appl Energy Mater* 2019, **2**:7655–7662, https://doi.org/10.1021/ACSAEM.9B01643/SUPPL_FILE/AE9B01643_SI_001.PDF.

In this study, $SnSe_2$ Nanorods on Carbon Cloth was synthesized which exhibited high selectivity, and activity towards electrochemical Reduction of CO_2. $SnSe_2$ nanorods selectively reduced CO_2 to formate with a high current density of 12.0 mA cm^{-2} and a high faradaic efficiency of 88.4% for formic acid at a low potential of–0.76 V (vs RHE).

116. Liu X, Yang H, He J, Liu H, Song L, Li L, Luo J, Liu XJ, He J, Liu HX, Song LD, Luo J, Yang H, Li L: **Highly active, durable ultrathin MoTe2 layers for the electroreduction of CO2 to CH4**. *Small* 2018, **14**:1704049, https://doi.org/10.1002/SMLL.201704049.

117. Ye J, Rao D, Yan X: **Regulating the electronic properties of MoSe2 to improve its CO2 electrocatalytic reduction performance via atomic doping**. *New J Chem* 2021, **45**:5350–5356, https://doi.org/10.1039/D0NJ05993E.

118. Yang X, Deng P, Liu D, Zhao S, Li D, Wu H, Ma Y, Xia BY, Li M, Xiao C, Ding S: **Partial sulfuration-induced defect and interface tailoring on bismuth oxide for promoting electrocatalytic CO2 reduction**. *J Mater Chem A* 2020, **8**:2472–2480, https://doi.org/10.1039/C9TA11363K.

119. Wang Y, Niu C, Zhu Y, He D, Huang W: **Tunable syngas formation from electrochemical CO2 reduction on copper nanowire arrays**. *ACS Appl Energy Mater* 2020, **3**:9841–9847, https://doi.org/10.1021/ACSAEM.0C01504/SUPPL_FILE/AE0C01504_SI_001.PDF.

120. Ma W, Xie S, Zhang XG, Sun F, Kang J, Jiang Z, Zhang Q, Wu DY, Wang Y: **Promoting electrocatalytic CO2 reduction to formate via sulfur-boosting water activation on indium surfaces**. *Nat Commun* 2019, **10**:1–10, https://doi.org/10.1038/s41467-019-08805-x. 2019 101.

121. Aljabour A, Coskun H, Zheng X, Kibria MG, Strobel M, Hild S, Kehrer M, Stifter D, Sargent EH, Stadler P: **Active sulfur sites in**

semimetallic titanium disulfide enable co2 electroreduction. *ACS Catal* 2020, **10**:66–72, https://doi.org/10.1021/ACSCATAL.9B02872/SUPPL_FILE/CS9B02872_SI_001.PDF.

122. Li H, Liu X, Chen S, Yang D, Zhang Q, Song L, Xiao H, Zhang Q, Gu L, Wang X: **Edge-exposed molybdenum disulfide with N-doped carbon hybridization: a hierarchical hollow electrocatalyst for carbon dioxide reduction**. *Adv Energy Mater* 2019, **9**:1900072, https://doi.org/10.1002/AENM.201900072.

123. Li J, Xu X, Huang B, Lou Z, Li B: **Light-Induced in situ formation of a nonmetallic plasmonic MoS2/MoO3-x heterostructure with efficient charge transfer for CO2Reduction and SERS detection**. *ACS Appl Mater Interfaces* 2021, **13**:10047–10053, https://doi.org/10.1021/ACSAMI.0C21401/SUPPL_FILE/AM0C21401_SI_001.PDF.

124. * Pellumbi K, Smialkowski M, Siegmund D, Apfel UP: **Enhancing the CO2 electroreduction of Fe/Ni-pentlandite catalysts by S/Se exchange**. *Chemistry* 2020, **26**:9938, https://doi.org/10.1002/CHEM.202001289.

In this study, the authors analyzed the effect of stepwise S/Se exchange in seleno-pentlandites $Fe_{4.5}$ $Ni_{4.5}S_8$–YSeY (Y = 1–5). It was observed that the existence of higher amount of selenium increased activity towards CO2RR. High Faradaic efficiency of 100% was observed for CO production at current density of 50 and 100 $mAcm^{-2}$. This work describes the tunability of the pentlandite based electrocatalysts for the CO_2 electrochemical reduction.

125. Wei X, Li Y, Chen L, Shi J: **Formic acid electro-synthesis by concurrent cathodic CO2 reduction and anodic CH3OH oxidation**. *Angew Chem Int Ed* 2021, **60**:3148–3155, https://doi.org/10.1002/ANIE.202012066.

126. Vass B Endrődi, Janáky C: **Coupling electrochemical carbon dioxide conversion with value-added anode processes: an emerging paradigm**. *Curr Opin Electrochem* 2021, **25**:100621, https://doi.org/10.1016/J.COELEC.2020.08.003.